NANO LETTERS

2007
Vol. 7, No. 2
264−268

Synthesis and Structural Characterization of Single-Crystalline Branched Nanowire Heterostructures

Yeonwoong Jung,† Dong-Kyun Ko,† and Ritesh Agarwal*

Department of Materials Science and Engineering, University of Pennsylvania, Philadelphia, Pennsylvania 19104

Received September 15, 2006; Revised Manuscript Received November 24, 2006

ABSTRACT

We report the synthesis of three-dimensional single-crystalline branched nanowire heterostructures, where the backbones and branches are assembled with ZnS and CdS, respectively. Growth of branch and backbones with control over the compositions was enabled via sequential seeding of gold nanocluster catalysts. Elemental mapping data confirmed that branched nanowire heterostructures were synthesized with the intended chemical modulation, CdS branches on ZnS backbones. Transmission electron microscopy studies showed that the growth of heterostructure branches occurs epitaxially from the backbone while maintaining single-crystalline structure. This unique class of heterostructures holds great potential in assembling electronics and photonics in three dimensions.

Low dimensional semiconductor nanowires are emerging as attractive building blocks for the assembly of electronic and optoelectronic device systems.[1−3] Fabrication of nanowire-based hierarchical systems is only meaningful if synthetic control over the morphology, position, and composition of nanowires is achieved. For example, in optoelectronic devices, control over the composition and diameter of nanowires allows for the tuning of the bandgaps of the materials, which determines the absorption and emission characteristics. The complexity and hence the functionality of the nanowire-based systems can be further enhanced by precisely controlling the morphology and structural parameters. Recently, synthetic methods have been reported to assemble three-dimensional branched and hyperbranched structures using a variety of materials and techniques including self-assembled dendritic growth of nanowires[4−6] and growth of multibranched nanowire structures via sequential seeding of catalysts.[7,8] The reported branched nanostructures, however, are compositionally uniform thereby limiting their functionalities. Assembly of more complex branched nanowire heterostructures with control over the nanowire backbone and branch compositions and dimensions can achieve unique functionalities similar to other reported nanowire axial[9−11] and core−shell heterostructures.[12] Recently, solution-based syntheses of tetrapod heterostructures were reported by Alivisatos and co-workers, where composition control was achieved over the different branches of the tetrapod.[13] However, gas-phase growth methods offers the ability to synthesize nanostructures with arbitrarily long branches[7,8] which can be subsequently used for device applications including interconnects. In the present study, we report the synthesis of single crystalline branched nanowire heterostructures, where the backbones and branches were assembled with ZnS and CdS materials respectively via the well-known vapor−liquid−solid (VLS) process.[14] The structure and the composition of the branched nanowire heterostructures were characterized by scanning and transmission electron microscopy (SEM, TEM) techniques, and it was observed that the CdS branches grow epitaxially from ZnS nanowire backbones. Branched nanowire homostructures assembled from ZnS and CdS were also synthesized to demonstrate the generality of our growth technique and to understand the structure of single crystalline branched II−VI nanowire materials.

Nanowires synthesized from II−VI materials are of particular interest primarily because of their wide range of optoelectronic properties. The spectrum of energy band gap of II−VI materials ranges from far-infrared to ultraviolet, and their heterostructures involve a wide range of band offsets, which adds variety and flexibility to band gap engineering.[15−17] Single crystalline CdS and ZnS nanowires have demonstrated attractive optical properties, which make them promising candidates for nanowire-based photonic applications, such as, nanoscale lasers,[18−20] waveguides,[21] and avalanche photodetectors.[22] Rational synthesis of CdS and ZnS nanowire heterostructures with control over their composition and morphology will allow for the assembly of complex nanowire-based systems. For example, branched

* Corresponding author. E-mail: riteshag@seas.upenn.edu.
† These authors made equal contribution in this study.

10.1021/nl0621847 CCC: $37.00 © 2007 American Chemical Society
Published on Web 12/21/2006

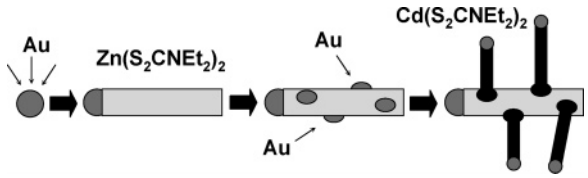

Figure 1. Schematic illustrating the synthesis of nanowire branched heterostructures. ZnS backbone nanowires are grown first via seeding of Au catalyst. CdS branch nanowires are then grown from secondary deposited Au catalyst on the previously grown ZnS nanowires.

nanowire heterostructures assembled with different materials on each branch and backbone are expected to be useful in nanowire-based smart optical waveguides and interconnects in three dimensions due to the inherent dimensionality of the structures, and multicolored light emitting diodes, and nanolasers obtained from single coherent structures.

Our growth method of ZnS (CdS) nanowires is based on metalorganic chemical vapor deposition (MOCVD) process using single molecular precursors, where zinc (cadmium) diethyldithiocarbamate ($Zn(S_2CNEt_2)_2$, $Cd(S2CNEt_2)_2$) is used to grow ZnS (CdS) nanowires.[23] The strategy to synthesize branched nanowire heterostructures is illustrated in Figure 1. First, the nanowire backbones with control over their composition and diameters were grown in a horizontal tube furnace with monodisperse gold nanoclusters (unconjugated Au sols, Ted Pella) as catalysts on Si substrate via the VLS method. $Zn(S_2CNEt_2)_2$ precursor was placed at the upstream side of the flow tube and the furnace temperature was slowly raised to 950 °C (substrate temperature ~850 °C). After the temperature of the furnace was stabilized, the precursor was slowly pushed into higher temperature zone of the furnace, and the nanowire growth was continued for 20 min. In the following step, the substrate was taken out of the furnace and was dipped into Au nanocolloids for secondary catalyst deposition and placed back into the furnace at the same position. Finally, the branched heterostructures were grown by introducing $Cd(S_2CNEt_2)_2$ precursor with the furnace temperature set at 740 °C (substrate temperature 660 °C). The rest of the procedure was same as that for ZnS nanowire growth. All the growths were carried out under Ar flow of 100 sccm at a base pressure of 300 Torr.

The morphology of the grown nanowires was examined using a scanning electron microscope (SEM) equipped in a dual beam focused ion beam system (FEI strata DB 235 FIB). Figure 2A shows a SEM image of ZnS nanowires which serve as backbones grown on a Si substrate by using Au nanocluster catalyst with an average diameter of 100 nm. The diameters of nanowires range approximately from 80 to 120 nm, and the nanowire lengths are typically greater than 10 μm. Further structural analysis of nanowires were performed using a 200 keV transmission electron microscope (TEM, JEOL 2010F). The lattice-resolved high-resolution TEM (HRTEM) image (Figure 2B) reveals that the ZnS nanowires are single crystalline and structurally uniform. The measured lattice spacing of 0.38 nm corresponds to the spacing between (100) planes as known from bulk ZnS

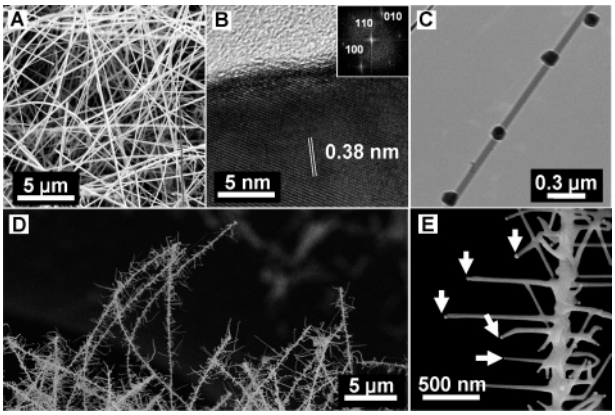

Figure 2. (A) SEM image of ZnS nanowire backbones. (B) HRTEM image of a ZnS nanowire and its corresponding two-dimensional Fourier transform (inset). (C) Low-magnification TEM image of Au catalyst deposited on ZnS nanowires. (D) SEM image of branched structures showing multiple branches spread out from each backbone nanowire. (E) SEM image of an isolated branched structure showing Au catalysts at the tips of the branches, marked by arrows.

samples. The reciprocal lattice peaks determined from two-dimensional Fourier transform of the image can be indexed to wurtzite-ZnS structure showing that the nanowire axis is aligned along the [100] direction, consistent with previous studies of ZnS nanowires.[24] TEM diffraction studies on a large number of individual ZnS nanowires also confirmed that the majority of the nanowires (>80%) grew along [100].

To enable the growth of branched nanowire heterostrucures, the as-grown ZnS nanowires on Si substrate were seeded with Au catalyst by dipping the substrate in Au colloidal solution followed by air-drying the sample. A low-magnification TEM image of a few isolated ZnS nanowires following Au catalyst deposition reveals dark particles attached to ZnS nanowires (Figure 2C). The particles were identified to be Au by energy-dispersive X-ray spectroscopy (EDS), indicating that Au nanoparticles were successfully deposited onto ZnS nanowires. The heterostructure branches were then grown by placing the ZnS nanowires with secondary catalyst deposited onto them in the growth furnace with a flow of CdS precursor materials. The growth conditions such as growth temperature and carrier gas flow rate were optimized to obtain good quality CdS branches on ZnS backbones. The branched nanowires were found to be densely grown on the Si substrate as observed in the SEM image (Figure 2D). Although precise control over the position of secondary Au catalysts on the backbone nanowires cannot be achieved, the density of branches on the backbone nanowires can be controlled by varying the concentration of Au colloid solution used to seed the branch growth (data not shown), which is also in agreement with other reported studies of branched homostructure nanowires.[7,8] At higher magnification (Figure 2E), the Au nanoparticles are clearly seen at the tips of the branches (marked by arrows in Figure 2E), with the diameter distribution of the branches being similar to the size distribution of the Au catalyst (40−70 nm). Supply of CdS precursors without secondary Au catalyst deposition leads to nonuniform coating of CdS on the pre-

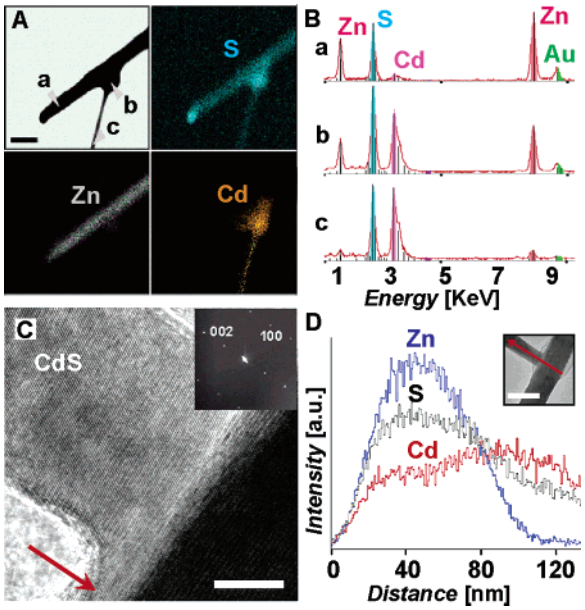

Figure 3. (A) STEM image of a branched nanowire heterostructure grown on a Mo TEM grid. Elemental mapping images of the branched nanowire indicate spatial distribution of Zn K, S K, and Cd L edges. Scale bar, 200 nm. (B) EDS point scanning data from the (a) backbone, (b) junction, and (c) branch regions of the nanowire marked in (A). (C) HRTEM image of the junction of a typical branched nanowire heterostructure. Scale bar, 10 nm. Crystalline shell structure of CdS is marked by the arrow. The inset is SAED obtained from the branch region. (D) EDS line scanning profile on the same nanowire across the junction region. Inset is a low-magnification TEM image of the nanowire with the EDS line scanning orientation specified. Scale bar, 100 nm.

existent ZnS nanowires without any indication of growth of CdS branches (Supplemental Information). This confirms that the growth of the branch nanowires is also based on the VLS mechanism and branching was initiated from the secondary deposited Au nanoparticles. The significant feature observed in the SEM image is that many branches possess preferred orientations with respect to the axis of the backbone nanowire (Figure 2E) with the branches exhibiting ~ 90° angles between the branch and the backbone axis. This observation indicates that most of the branches possess a defined relation with respect to the crystalline structure of the backbone. However, as seen in Figure 2E, a very small number of branches do not exhibit a 90° angle with respect to the backbone nanowire (most likely due to structural defects at the junction region) and they tend to fuse with other branches. Detailed structural analysis of branched nanowire heterostructures will be discussed later in the paper.

Chemical composition analysis was conducted with EDS in scanning TEM (STEM) using a 0.7 nm sized probe to examine if the branched nanowires were grown with chemical compositions as intended, i.e., ZnS backbone and CdS branches. To enable the analysis of the structures with minimum structural damage, the branched nanowire heterostructures were directly grown on Mo TEM grid with the same conditions as mentioned above. The EDS elemental mapping images of a branched nanowire heterostructure are shown in Figure 3A to identify the spatial distributions of Zn, Cd, and S in the backbone and branches. In the backbone region, a strong Zn K edge is detected, while the Cd signal is barely visible. In contrast, a Cd L edge signal is dominant in the branch region, while the Zn K edge signal is nearly absent. The signal of the S K edge is uniformly distributed over the entire structure as expected. The weak S K edge signal from the branch region is due to the smaller diameter (~40 nm) of the branch compared to that of the backbone (~120 nm).

Quantitative analysis of the chemical compositions was further performed by EDS point scanning using a nanometer-sized probe (Figure 3B) on three different regions specified in Figure 3A, i.e., (a) backbone, (b) junction, and (c) branch. In the backbone region (a), Zn and S peaks are dominant while the Cd peak intensity is negligible. The Zn and S are present in the expected stoichiometric ratio (% Zn = 52.3; % S = 47.7) Similar energy spectra were consistently observed on every randomly selected spot throughout the backbone region. The EDS data from the junction region (b) reveals that Zn and Cd peaks are at similar heights, implying that an alloyed state of Cd_xZn_{1-x} is obtained locally due to the interdiffusion of Zn and Cd. In the branch region (c), stoichiometric composition of Cd and S was also detected (% Cd = 48.9; % S = 51.1) with a negligible Zn peak. This study clearly suggests that backbone and branched regions of the nanowires are indeed ZnS and CdS nanowires, respectively, with a certain level of interdiffusion of Zn and Cd at the junction region.

Structural analysis of the branched nanowire heterostructure junction was performed by HRTEM (Figure 3C). Significantly, the HRTEM image shows that the entire junction region is single crystalline without showing any obvious structural defects. The crystalline structure of CdS branch (bright part) continues into the junction region (dark part) where the alloyed state of $Cd_xZn_{1-x}S$ is formed. Interestingly, a local thin crystalline shell of CdS was typically observed at the heterojunction region as indicated by an arrow in Figure 3C, which resulted in a slightly thicker interfacial region (as seen in Figure 3). The selective area electron diffraction (SAED) pattern obtained from the branch region shows that the CdS branch possess single crystalline wurtzite structure with the branch axis aligned along a [002] orientation, consistent with previous studies of CdS nanowires.[25,26] SAED patterns obtained from different parts of the branched heterostructure (backbone and alloyed junction) also revealed reciprocal lattice peaks similar to that of the branch region, suggesting that the branched heterostructure is crystalline throughout the entire structure. Previous studies of alloyed $Cd_xZn_{1-x}S$ nanowires have shown that single crystalline structures are possible throughout the alloyed nanowire.[27] It is possible that the compositional variation across the junction can relieve strain due to relatively large lattice mismatch between CdS and ZnS (~8%), therefore forming single crystalline junctions without obvious structural defects. The consistently observed 90° angle between the branch and the backbone and the observation of single-crystalline junction region suggest that the CdS branches grow epitaxially from the crystallographic planes of the ZnS backbone that lie in the [100] zone axis. The sparsely

observed oblique branches are attributed to the various crystal misorientations and defects at the junctions, such as twins and stacking faults (data not shown).

The chemical composition in the vicinity of the junction region was studied by EDS line scanning experiments performed on the nanowire shown in Figure 3C, with the line scanning conducted across the backbone along the length of the branch (scanning direction shown in Figure 3D inset). A chemical composition profile of Zn, Cd, and S was recorded as a function of distance, revealing spatial distribution of Cd and Zn along the scanned region (Figure 3D and inset). The backbone region (first 0−100 nm region) up to the physical junction where the branch starts shows that the Zn peak is higher than the Cd peak. The presence of Cd in this region is due to the observed shell structure of CdS and also attributed to the diffusion of Cd into the backbone, thus, forming an alloyed state of $Cd_xZn_{1-x}S$ where x varies along the scanning orientation. In the branch region (after ∼100 nm in scanning distance), the Cd peak is observed to be relatively much higher than the Zn peak and eventually the Zn signal disappears after 120 nm. The presence of the small Zn content in the first 20 nm of the branch region is attributed to Zn diffusion from the backbone toward the branch region. It is worth mentioning that the extent of alloying can be controlled with the temperature used during the branch growth, with higher furnace temperatures (above ∼780 °C) forming an alloyed region over 150 nm and lower furnace temperatures (below ∼700 °C) not producing single crystalline junctions. The alloyed region observed in our heterostructures is comparable to many reports of nanowire-based heterostructures in different geometries.[11,12,28] Further experiments are being performed to obtain better control over the chemical composition of the branched heterojunctions.

To further understand the structure of branched II−VI semiconductor nanowires and to demonstrate the generality of the growth scheme, branched homostructure nanowires (backbone and branch are same materials) were synthesized from ZnS and CdS materials. For ZnS homostructures, branches and backbones were grown at 950 °C (furnace temperature), and CdS homostructures were grown at 765 °C (furnace temperature) at the same flow rate and base pressure mentioned before. Parts A and B of Figure 4 are SEM images of ZnS branched nanowires showing that multiple branching was realized on backbone nanowires. Au catalysts were also observed at the ends of the branches confirming that the branch growth occurred via the VLS mechanism. Significantly, there exists a defined relationship between the orientation of the branches and the axis of the backbone, with the angles between the branches and the backbone varying within a very narrow range (approximately ∼120°), sharply in contrast to the ∼90° angle observed in the case of CdS/ZnS heterobranched nanowires. Figure 4C is a low-magnification TEM image of an isolated CdS branched nanowire displaying an ∼120° angle between the branches and the backbone. The lattice-resolved HRTEM images of the junction regions of the ZnS (Figure 4D) and CdS (Figure 4E) branched nanowires clearly suggest that these branched nanowires have single crystalline structure throughout the

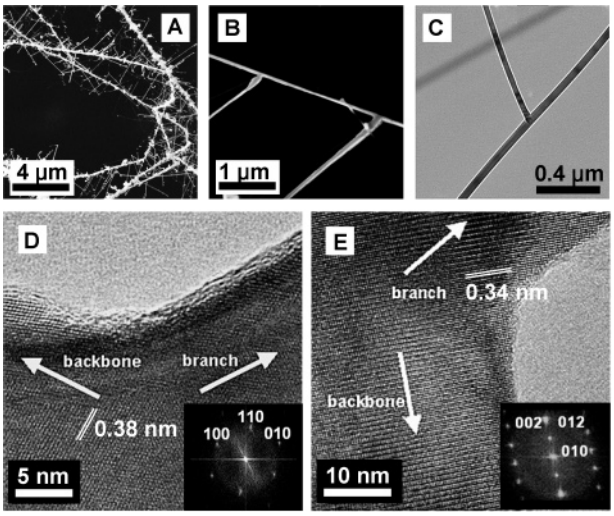

Figure 4. Branched homostructure nanowires (A, B) SEM images of ZnS branched homostructure nanowires showing multiple branches grown on the backbones with ∼120° angles between the branches and the backbone. (C) Low magnification TEM image of a CdS branched homostructure nanowire. HRTEM images of the junction of (D) ZnS, and (E) CdS branched homostructure nanowires. The insets are two-dimensional Fourier transform of the corresponding TEM images.

branch, backbone, and the junction with a clean interface between the backbone and the branch. The indexed reciprocal lattice peaks obtained from the Fourier transforms of the respective images display the crystalline orientation of each branch and backbone (Figure 4D,E). The ZnS branched nanowire has the backbone axis along the [100] direction (as discussed earlier) and the branch axis along [010], with measured lattice spacing determined to be 0.38 nm corresponding to (100) crystal planes. The crystal orientations of the backbone and branch indicate that the angle between the backbone and the branch is ∼120° as observed in ZnS homostructures. For CdS branched nanowire, the indexed reciprocal lattice peaks and the lattice spacing of 0.34 nm indicate that the backbone is aligned along the [002] direction, while the branch is aligned along the [012] direction, in agreement with the ∼120° angle observed between the backbone and branches. The above analysis suggests that ZnS and CdS nanowire branches grow epitaxially in agreement with previous studies of branched nanowire structures assembled from III−V and group IV semiconductors.[7]

The structural analysis discussed above provides meaningful insights into the mechanism of the branch growth in the branched nanowire heterostructures. The clean interface at the junction in the branched homostructure is distinct from the junction of the branched heterostructures where a thin shell (typically <10 nm) of the secondary material on the backbone is observed locally, leading to a distinct interfacial region (Figure 3C). This shell structure can be understood by considering that the surface of the backbone nanowire acts as a substrate where the two chemically different species (ZnS and CdS) with a large lattice mismatch interact. The Au catalyst deposited on the backbone nanowires acts as nucleation sites to collect the secondary material (CdS) which

forms an eutectic melt with Au. The collected material then undergoes structural relaxation during its growth to overcome the lattice mismatch by forming structures of intermediate chemical compositions of $Cd_{1-x}Zn_xS$. Finally, the local shell structure results on the surface of the backbone nanowire, which enables the secondary material to grow into a branched structure while maintaining its crystalline structure without structural defects. For the case of homobranched nanowires, the secondary material grows following the same crystallography of the backbone nanowire resulting in a clean junction, since it is chemically and structurally identical to the backbone material. However, more detailed experiments such as in situ TEM characterization are necessary to elucidate the exact mechanism of the branch heterostructure growth, which will be a potentially interesting research subject in nanostructure growth studies.

In conclusion, we have successfully synthesized branched nanowire heterostructures based on the VLS mechanism via sequential seeding of catalysts. The chemical composition analysis by EDS-TEM study confirms that branched heterostructures were successfully synthesized from ZnS and CdS. Electron microscopy studies indicate that the growth of heterostructure branches occurs epitaxially while maintaining single crystalline structure. This new nanowire heterostructure, distinct from nanowire axial,[9−11] and radial heterostructures,[12,28] will be useful as nanoelectronic and photonic building blocks to control the generation and transportation of carriers and photons in three dimensions.

Acknowledgment. This work was supported by the startup grants from the University of Pennsylvania, and funds from the University of Pennsylvania Research Foundation (URF).

Supporting Information Available: SEM images of as-grown ZnS nanowires and ZnS nanowires after CdS precursor supplied without secondary Au catalyst deposition and a low-magnification TEM image of a ZnS nanowire after CdS precursor is supplied without secondary Au catalysts. This material is available free of charge via the Internet at http://pubs.acs.org.

References

(1) Lieber, C. M. *MRS Bull.* **2003**, *28*, 486.
(2) Samuelson, L. *Mater. Today* **2003**, *6*, 22.
(3) Xia, Y.; Yang, P.; Sun, Y.; Wu, Y.; Mayers, B.; Gates, B.; Yin, Y.; Kim, F.; Yan, H. *Adv. Mater.* **2003**, *15*, 353.
(4) Yan, H.; He, R.; Johnson, J.; Law, M.; Saykally, R. J.; Yang, P. *J. Am. Chem. Soc.* **2003**, *125*, 4728.
(5) Zhou, J.; Ding, Y.; Deng, S. Z.; Gong, L.; Xu, N. S.; Wang, Z. L. *Adv. Mater.* **2005**, *17*, 2107.
(6) May, S. J.; Zheng, J.-G.; Wessels, B. W.; Lauhon, L. J. *Adv. Mater.* **2005**, *17*, 598.
(7) Wang, D.; Qian, F.; Yang, C.; Zhong, Z. H.; Lieber, C. M. *Nano Lett.* **2004**, *4*, 871.
(8) Dick, K. A.; Deppert, K.; Larsson, M. W.; Martensson, T.; Seifert, W.; Wallenberg, L. R.; Samuelson, L. *Nat. Mater.* **2004**, *3*, 380.
(9) Gudiksen, M. S.; Lauhon, L. J.; Wang, J.; Smith, D.; Lieber, C. M. *Nature* **2002**, *415*, 617.
(10) Bjork, M. T.; Ohlsson, B. J.; Sass, T.; Persson, A. I.; Thelander, C.; Magnusson, M. H.; Deppert, K.; Wallenberg, L. R.; Samuelson, L. *Nano Lett.* **2002**, *2*, 87.
(11) Wu, Y.; Fan, R.; Yang, P. *Nano Lett.* **2002**, *2*, 83.
(12) Lauhon, L. J.; Gudiksen, M. S.; Wang, D.; Lieber, C. M. *Nature* **2002**, *420*, 57.
(13) Milliron, D. J.; Hughes, S. M.; Cui, Y.; Manna, L.; Li, J.; Wang, L.-W.; Alivisatos, A. P. *Nature* **2004**, *430*, 190.
(14) Wagner, R. S.; Ellis, W. C. *Appl. Phys. Lett.* **1964**, *4*, 89.
(15) Mcclean, I. P.; Thomas, C. B. *Semicond. Sci. Technol.* **1992**, *7*, 1394.
(16) Artemyev, M. V.; Sperling, V.; Woggon, U. *J. Appl. Phys.* **1997**, *81*, 6975.
(17) Falcony, C.; Garcia, M.; Ortiz, A.; Alonso, J. C. *J. Appl. Phys.* **1992**, 721525.
(18) Duan, X.; Huang, Y.; Agarwal, R.; Lieber, C. M. *Nature* **2003**, *421*, 241.
(19) Ding, J. X.; Zapien, J. A.; Chen, W. W.; Lifshitz, Y.; Lee, S. T.; Meng, X. M. *Appl. Phys. Lett.* **2004**, *85*, 2361.
(20) Agarwal, R.; Barrelet, C. J.; Lieber, C. M. *Nano Lett.* **2005**, *5*, 917.
(21) Law, M.; Sirbuly, D.; Johnson, J.; Goldberger, J.; Saykally, R.; Yang, P. *Science* **2004**, *305*, 1269.
(22) Hayden, O.; Agarwal, R.; Lieber, C. M. *Nat. Mater.* **2006**, *5*, 352.
(23) Barrelet, C. J.; Wu, Y.; Bell, D. C.; Lieber, C. M. *J. Am. Chem. Soc.* **2003**, *125*, 11498.
(24) Xiong, Q.; Wang, J.; Reese, O.; Lew, L. C.; Voon, Y.; Eklund, P. C. *Nano Lett.* **2004**, *4*, 1991.
(25) Kar, S.; Chaudhuri, S. *J. Phys. Chem. B* **2006**, *110*, 4542.
(26) Ge, J.-P.; Wang, J.; Zhang, H.-X.; Li, Y.-D. *Chem. Eur. J.* **2004**, *10*, 3525.
(27) Hsu, Y.-J.; Lu, S.-Y.; Lin, Y.-F. *Adv. Funct. Mater.* **2005**, *15*, 1350.
(28) Qian, F.; Gradecak, S.; Li, Y.; Wen, C.; Lieber, C. M. *Nano Lett.* **2005**, *5*, 2287.

NL0621847